Discontinuity thermal stresses at the juncture of cylindrical shell and spherical head

Aly A. Helmy [a], A. M. Raafat [a] and M. E. Haroun[b]

[a]*Mechanical Eng. Dept., Faculty of Eng., Alexandria University, Alexandria, Egypt*
[b]*Jabco oil company, Alexandria , Egypt*

The wide spectrum of applications of pressure vessels, consisting of different shell shapes intersecting together and subjected to mechanical and thermal loading as in nuclear power plants and chemical reactors, makes the study of the discontinuity stresses at the juncture of vessel parts is of major importance. Serious failures of such pressure vessels may occur because of thermal shock, thermal creep or due to thermal cycles. Hence, in this paper, the discontinuity stresses produced at the juncture of cylindrical shell and spherical head due to time dependent thermal gradient, have been evaluated. The finite element software (COSMOS) is applied to determine the temperature profiles as well as the associated deformations. The results show that the maximum hoop stresses occur at an early stage of the thermal transient. Also, it was found that the larger the time elapsed, the less are the hoop stresses. On the other hand, it was found that the discontinuity stresses produced at the vessel juncture depend totally on the shell mean temperature.

إن الاستخدام الواسع لاوعية الضغط، المكونة من قشريات متصلة ومعرضه لاحمال ميكانيكية وحرارية كما فى محطات توليد الطاقة النووية أو المفاعلات الكيميائية، يجعل من دراسة الاجهادات المتولدة عند منطقة تقاطع تلك القشريات ذو اهمية كبرى. وذلك حيث يحدث انهيار لاوعية الضغط ناتج من الصدمات الحرارية او الزحف اوالاحمال الحرارية المتكررة. فى هذا البحث تمت دراسة الاجهادات الناتجة من وجود تدرج حرارى متغير مع الزمن عند منطقة تقاطع اسطوانة قشرية وغطاء نصف كروى. وقد تم استخدام برنامج OSMOS الذى يقوم بحساب التوزيع الحرارى خلال سمك الاسطوانة والنصف كرة وكذلك حساب التشكلات الناتجة بهما باستخدام طريقة العناصر المحددة. وقد عرضت النتائج التى تم الحصول عليها فى جداول ومنحنيات. هذا وقد اظهرت تلك النتائج ان اقصى اجهادات تحدث فى مرحلة مبكرة من مراحل التدرج الحرارى. كما اظهرت النتائج ان الاجهادات تقل بمضى زمن التدرج الحرارى حتى تصل لاقل قيمة لها فى حالة تدرج حرارى ثابت.

Keywords: Thermal stresses, Cylindrical shell, Spherical head, Discontinuity stresses, Finite element

1. Introduction

The first general shell theory was not developed until 1888 by Love. Subsequently, many efforts have been directed towards the improvement of Love's formulation in order to treat applications of practical interests, as may be found in texts by Flügge [1] and Kraus [2] among others.

In industry, pressure vessel design is rather relying on design codes than it does on stress analysis. On the other hand, most of these codes provide very brief guide lines for the design of cases involving discontinuity stresses due to thermal gradient at pressure vessels excluding any computational techniques.

The mathematical expressions determining the stresses and displacements of cylinders and spheres have been given by Timoshenko [3]. His formulation represents the foundation of the evaluation of the thermal stresses and the associated deformations for any temperature function that can be analytically expressed.

Harvey [4] introduced the significance of thermal stresses in cylindrical shells. He also presented the analogy between a pressurized cylinder and a beam on elastic foundation theory. This concept has been implemented successfully for determining the discontinuity stresses at a cylindrical shell intersected with different ends.

As analytical solutions of thin shell structural problems are limited in scope and in general do not apply to arbitrary shapes, loading, stiffness, irregularities and many other aspects of practical interests, so numerical

techniques come to the fore as an efficient approach to thin shell structure analysis. The finite element method has been introduced in transient heat conduction problems by Wilson and Nickell [5]. On the other hand, reviews made by Gallagher [6] and Knowles et al. [7] provided an excellent prospective of the efforts in the analysis of shells by finite element method. The shape of the element used in finite element analysis plays an important role in the analysis. One of the most distinct efforts was made by Ahmed et al. [8], who has derived the general formulation for a curved element along with the reduced integration technique. A comprehensive demonstration of curved elements with the necessary translation between different coordinates was given by Zienkiewicz et al. [9] and [10]. Han et al. [11] adopted the doubly curved element in cartesian coordinates system for both the geometry and displacement.

The problem of a sphere-cylinder intersection can be analyzed by different methods. M. Fayed [12] proposed a modified finite difference meshing scheme to evaluate the discontinuity stresses at the intersection of a sphere and a cylinder of different thicknesses. On the other hand, the efficiency of the finite element formulation encouraged the continuous progress in dealing with situations of more theoretical complexity but of practical interests. Godoy and Croll [13] studied the problem of the geometrical discontinuity in thin elastic shells having meridional disturbance, by using the finite element technique.

The solution of transient heat conduction problems are obtained by different numerical techniques, however, the application of the finite element method to heat conduction analysis has attracted considerable attention since the procedure was first reported by Zienkiewicz and Cheung [14]. Warzee [15] presented a solution for the unsteady state heat conduction through two different techniques, the finite element and the Laplace transformation. Also, Karan and Perwez [16] reported a specified formulation to handle heat conduction problems in a thin axisymmetric shell. The heat transient occurs in the test loop of a fast breeder reactor during fuel element shutdown was studied by F. Cecari et al. [17]. A case study of how does the finite element technique can be used in field problem was presented by Duijvesign et al. [18] on the failure process of a reactor pressure vessel lower spherical head due to contact with the molten core material. Also, Vilhelmsen [19] used the finite element method to study the integrity of flat end to cylinder shell connections operating in the creep regime. The thermal stresses which occur in pressure vessels exposed to through wall temperature gradients was studied by Law et al. [20]. The resulting response was calculated using finite element software. On the other hand, a general analysis of one dimensional steady-state thermal stresses in a hollow cylinder made of functionally graded material was studied by Jabbaria et al. [21].

In the present study, the maximum membrane and discontinuity stresses produced in a cylinder, sphere and their juncture while they are under time dependent thermal gradient have been represented. A finite element model which constitutes a two dimensional plane element was utilized to construct the temperature profiles and to evaluate the radial displacements of a cylinder and a sphere closure through the available finite element software "COSMOS-M". The resulting displacements were then introduced into the evaluated formulation in order to define the discontinuity stresses.

2. Model

Thermal transient problems usually involve the determination of the temperature profile in space as well as the temperature evolution through time domain. However, during thermal transient, the thermal gradient through the shell wall cannot be simply expressed and analytical solutions for the resulted thermal stresses could not be obtained. In order to overcome these difficulties, the temperature profiles based on the known transient heat transfer Heisler's chart solutions [22] are obtained for a limited number of cases, then compared to the corresponding finite element model outputs resulted by the finite element software package.

Upon confirming the concurrence of both results, comprehensive finite element models run through the software while varying the thermal parameters. The numerical results

have then been examined to achieve the following objectives of studying thermal state:

- Determining the maximum temperature difference across the shell wall and its occurrence.

- Interim mapping the temperature profiles during the thermal transient.

- Evaluation of the maximum membrane and discontinuity thermal stresses.

- Evaluation of the radial growth during thermal cycle.

The following assumptions are considered:

- The shells are thin.

- Heat loading is axisymmetric with respect to circumferential direction of the shell and no axial thermal gradient exists.

- The shell material properties as modulus of elasticity, thermal conductivity and coefficient of thermal expansion remain constant throughout the proposed temperature regimes.

- The shell outer surface is to be perfectly insulated where as the inner one is being subjected to a hot fluid flow of varying temperature T_∞ and convection coefficients h.

- Elastic state of stress that is in full adherence with Hook's law.

Applying the following stress–strain relations at a point in a cylinder subjected to temperature variations [3];

$$\varepsilon_r = \frac{1}{E}\left(\sigma_r - \nu(\sigma_\theta + \sigma_z)\right) + \alpha T ,$$

$$\varepsilon_\theta = \frac{1}{E}\left(\sigma_\theta - \nu(\sigma_z + \sigma_r)\right) + \alpha T ,$$

$$\varepsilon_z = \frac{1}{E}\left(\sigma_z - \nu(\sigma_\theta + \sigma_r)\right) + \alpha T ,$$

and assuming that the cylinder is sufficiently long so that plane strain conditions may be assumed, i.e $\varepsilon_z = 0$, then:

$$\sigma_z = \nu(\sigma_r + \sigma_\theta) - \alpha E T ,$$

so the stress strain relations become:

$$\varepsilon_r = (1+\nu)\alpha T + \left(\frac{1-\nu^2}{E}\right)\left(\sigma_r - \frac{\nu}{1-\nu}\sigma_\theta\right),$$

$$\varepsilon_\theta = (1+\nu)\alpha T + \left(\frac{1-\nu^2}{E}\right)\left(\sigma_\theta - \frac{\nu}{1-\nu}\sigma_r\right),$$

and by applying the following boundary conditions;

$$\sigma_r = 0 \quad \text{at r = a, r = b,}$$

we can finally get the radial stress;

$$\sigma_r = \frac{\alpha E}{(1-\nu)}\frac{1}{r^2}\left[\frac{(r^2-a^2)}{(b^2-a^2)}\int_a^b Trdr - \int_a^r Trdr\right] ,$$

the hoop stress;

$$\sigma_\theta = \frac{\alpha E}{(1-\nu)}\frac{1}{r^2}\left[\frac{(r^2+a^2)}{(b^2-a^2)}\int_a^b Trdr + \int_a^r Trdr - Tr^2\right]$$

and the longitudinal stress;

$$\sigma_z = \frac{\alpha E}{(1-\nu)}\left[\frac{2}{(b^2-a^2)}\int_a^b Trdr - T\right].$$

While the radial displacement may be given by:

$$U_r = \frac{\alpha}{r}\frac{(1+\nu)}{(1-\nu)}\left[\int_a^r Trdr + \frac{(1-2\nu)r^2+a^2}{(b^2-a^2)}\int_a^b Trdr\right],$$

where *a* and *b* represent the inner and outer radii, respectively.

Similarly, for a hollow sphere under radial temperature variation, the radial stress may be given as:

$$\sigma_r = \frac{2E\alpha}{(1-\nu)}\left[\frac{r^3-a^3}{(b^3-a^3)r^3}\int_a^b Tr^2dr - \frac{1}{r^3}\int_a^r Tr^2dr\right],$$

and the hoop stress is given by;

$$\sigma_\theta = \frac{2E\alpha}{(1-v)}\left[\frac{2r^3+a^3}{2(b^3-a^3)r^3}\int_a^b Tr^2\,dr + \frac{1}{2r^3}\int_a^r Tr^2\,dr - \frac{1}{2}T\right],$$

while the radial displacement is given by;

$$U_r = \frac{\alpha}{r^2(1-v)}$$

$$\left[(1+v)\int_a^r Tr^2\,dr - \frac{2r^3(1-2v)+a^3(1+v)}{a^3-b^3(1-2v)}\int_a^b Tr^2\,dr\right].$$

One dimensional unsteady state heat conduction with convection boundary have been taken into consideration for thermal transient case. The convection boundary is proposed to be produced by the passage of a hot fluid of temperature T_∞. The convection film coefficient h and the fluid temperature values are varied in order to examine their effects on the propagation of the discontinuity stresses. However, in thermal transient, the temperature gradient through the vessel wall cannot be simply expressed. Moreover, the time at which the maximum temperature difference across the vessel wall takes place, remains analytically not found. To overcome such difficulty, the finite element software was used to construct the temperature profile during thermal transient, while the results of the finite element model obtained was utilized to establish simplified approach as proposed by Harvey [4] to calculate the stresses associated with the maximum thermal stresses.
If a solid body is suddenly subjected to a temperature change, some time must be elapsed before an equilibrium temperature condition prevails in the body. Fig. 1 represents a hypothetical temperature distribution progress through the cylinder wall during time intervals t_n till the reach of the steady state. The hollow cylinder will be considered with perfectly insulated exterior surface, while the interior one is suddenly exposed to a hot fluid of known temperature T_∞.

3. Results and discussion

The physical and the mechanical properties of both the cylindrical shell and spherical
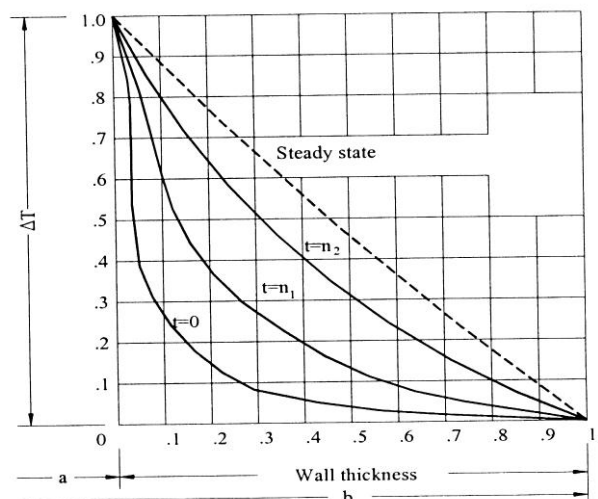

Fig. 1. The hypothetical temperature distribution rogress during time intervals t_n.

head used in calculations, in accordance with the code of pressure vessels ASME SEC 8 DIV. 2, are as follows:
Material: Carbon steel (ASTM 516 GR. 70)
Elastic modulus E: 210 GPa
Poisson's ratio v: 0.28
Coefficient of thermal expansion α: $1.3*10^{-5o}$ K^{-1}
Thermal Conductivity K: 43 W/m °K
Shell inner diameter: 2133 mm
Shell outer diameter: 2301 mm
Shell thickness: 84 mm
On the other hand, the cylindrical shell axial length was taken as in most practical cases, where the length of the cylinder should exceed the attenuation (decay) length $\left(2.45\sqrt{\text{shell radius}\times\text{shell thickness}}\right)$ [23].

Figs. 2 and 3 illustrate the numerical temperature history, for different convection coefficients and constant ambient temperature, of two opposite nodes across the cylinder and sphere walls through thermal transient, respectively. The thermal boundary conditions used in plotting both figures are:

Convection coefficient h: 40, 80,..., 200 W/m^2 K
T_∞ (fluid): 560 K
Initial temperature T_i: 293 K.

The previous figures show that the maximum temperature differences across the cylinder and sphere walls take place at a very early stage of the thermal transient (300 s).
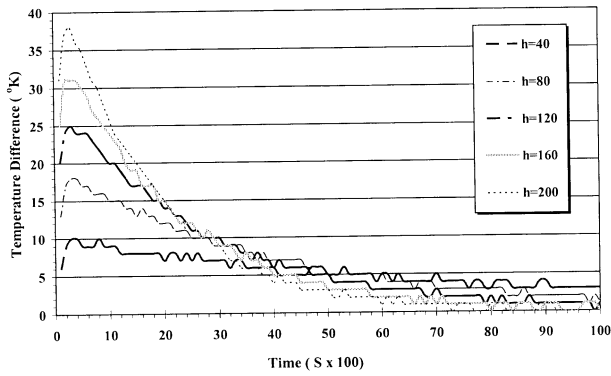
Fig. 2. Temperature distribution between two opposite nodes across the cylinder wall at different convection coefficients.
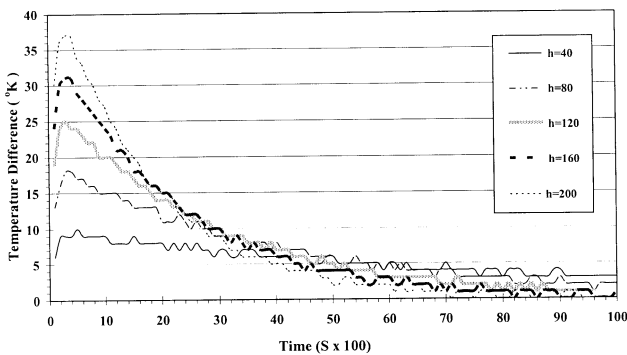

Fig. 3. Temperature distribution between two opposite nodes across the sphere wall at different convection coefficients.

It is also apparent from the previous figures, that the elapsed time to reach the maximum temperature differences remains almost constant for all the values of the film coefficients. This conclusion is however confined to specific shell material properties as thermal conductivity and thickness. The figures may also indicate that the magnitudes and occurrence of the maximum temperature difference across both cylinder and sphere are almost similar.

The temperature profiles across the cylindrical shell wall for a wide range of convection coefficients were given by the finite element software COSMOS. These profiles show that the higher the coefficient is, the larger is the temperature difference through the wall thickness and the steeper are the resulted temperature profiles. A comparison between these thermal profiles and the profiles given by Heisler's charts as given in fig. 4 shows well
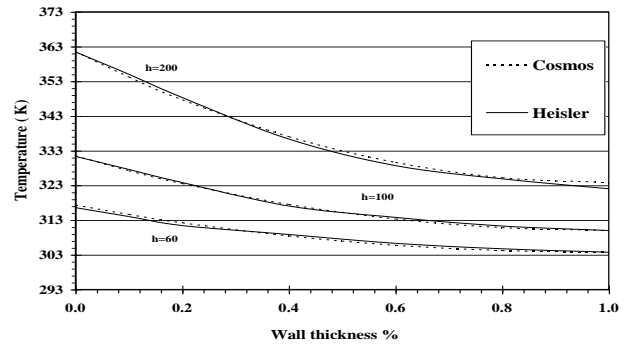

Fig. 4. Temperature profiles calculated by heisler charts versus finite element results for different convection coefficients.

matching. On the other hand, a curve-fitting procedure was adopted for the temperature profiles giving second degree polynomials with which the average temperature of the entire vessel wall was established.

This procedure was repeated for different fluid temperatures T_∞ and the average value of the temperature which represents the mean value throughout the entire wall thickness may be given by:

$$T_{av} = \frac{\left(T_\infty - 273\right)}{A}.h + \left(T_i + 3\right).$$

Where;
A is constant = 1352, and
T_i is the initial temperature, K.

The average temperature was used to evaluate the integrals in the stress and displacement equations according to the approach adopted by Harvey [4].

Table 1 lists a comparison between the maximum transient hoop stresses at the cylinder inner and outer walls calculated numerically and analytically. From the table we may conclude that the maximum error does not exceed 9%.

Fig. 5 shows the development of the membrane hoop stresses at the cylinder shell during thermal transient is plotted on an interim basis starting from maximum thermal transient (300 s).

Examining the plotted data given in fig. 5 along with the temperature numerical values listed in table 2 indicates that the hoop stresses have their maximum values at the early stage of the thermal cycle, then deplete with time. Moreover, the maximum hoop

Table 1
Maximum transient hoop stresses

Coefficient (h)	Inner surface			Outer surface		
W/ m² K	numerical	analytical	error %	numerical	analytical	error %
40	-24.1	-24.6	2	11.4	11.6	2
80	-45.4	-45.5	0	21.5	23.13	8
120	-64.6	-61.8	4	30.6	33	8
180	-89.6	-86.5	3	42.6	46.3	9
200	-97.1	-95.6	2	46.2	48.5	5

stresses are totally dependent on the absolute temperature difference between the vessel inner and outer surface.

The development of the discontinuity hoop and meridional stresses throughout the thermal cycle is shown in figs. 6, 7.

The positive values of the x-axis represent a distance at a line on the cylinder surface parallel to its axis, while the negative values represent a straight distance on the sphere circumference starting at the sphere-cylinder juncture towards the sphere apex.
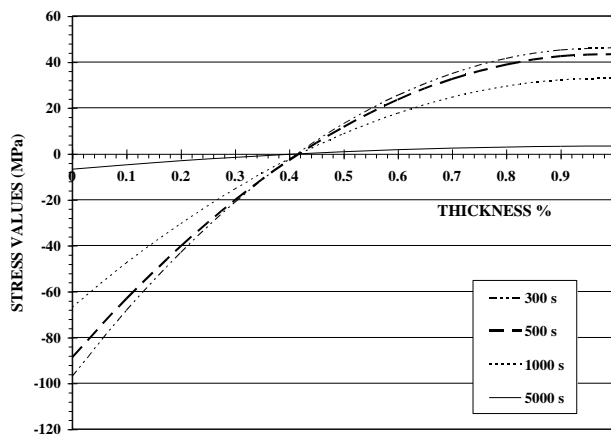

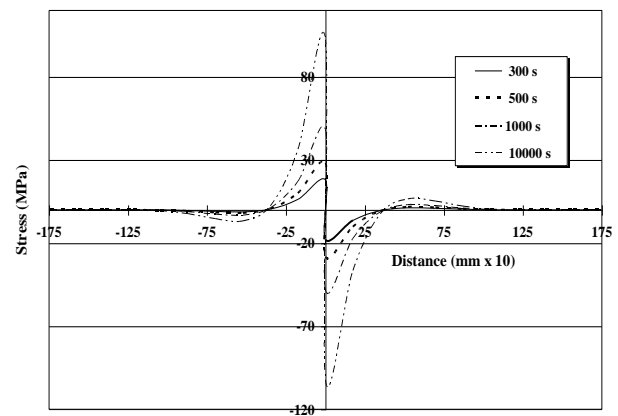Fig. 5. Hoop stresses during thermal transient.

Fig. 6. Development of discontinuity hoop stresses during thermal transient.

Table 2
Temperature difference between inner and outer surfaces

Elapsed time (s)	300 s	500 s	1000 s	5000 s
Inner wall temp. (K)	362	384	428	548
Outer wall temp. (K)	324	349	402	545
Temperature difference	38	35	26	3

Table 3
Displacement and maximum discontinuity stresses

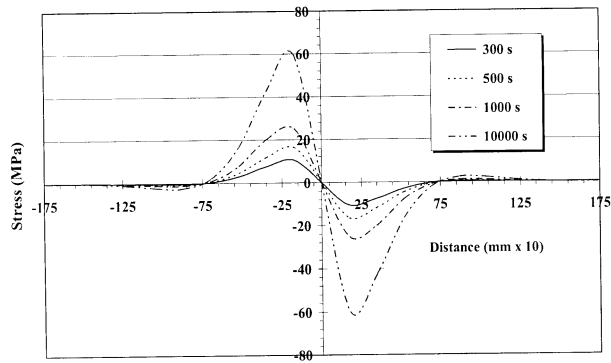| Elapsed time (s)	t_a K	t_b K	Temperature difference K	Cylinder displacement (mm)	Sphere displacement (mm)	Displacement difference (mm)	Discontinuity hoop stresses MPa	Discontinuity meridional stresses MPa
300	362	324	38	0.798	0.608	0.19	18	10.5
500	384	349	35	1.25	0.952	0.297	28.2	16.5
1000	428	402	26	2.17	1.66	0.511	48.3	25.2
10000	560	560	0	4.93	3.85	1.08	102.3	59.8

Fig. 7. Development of discontinuity merdional stresses during thermal transient.

The figures show that the discontinuity thermal stresses (hoop and meridional) increase with the elapsed time and have its maximum value at the end of the thermal cycle irrespective of the temperature differences across the wall, as shown in table 3, from which it is clear that the discontinuity thermal stress is proven to be totally dependent on the sphere-cylinder displacement difference no matter the across-shell wall-temperature difference is.

4. Conclusions

From the results shown previously we may conclude that:
- The membrane maximum hoop stresses occurs at the early stage of thermal transient where the maximum across-the-wall temperature difference takes place, irrespective of the shell mean temperature.
- The larger the time elapsed, the less are the hoop stresses, which approach their minimum values at the steady state.
- Unlike the membrane stresses, discontinuity stresses induced at the vessel juncture as a result of displacement conflict, are totally dependent on the shell mean temperature no matter the across-the-shell wall-temperature difference is.

Nomenclature

a, b	are the inner and outer shell radii,
E	is the young's modulus,
h	is the convection coefficient,
K	is the thermal conductivity,
r	is the radius of an arbitrary point,
t	is the time,
t_a, t_b	is the temperatures at juncture shell walls,
T	is the temperature at an arbitrary point,
T_i	is the initial temperature,
T_{av}	is the average temperature,
T_∞	is the fluid temperature, and
U_r	is the radial displacement due to temperature.

Greek symbols

α	is the coefficient of linear thermal expansion,
ΔT	is the temperature difference,
$\varepsilon_r \, \varepsilon_\theta \, \varepsilon_z$	are the strain in radial, tangential & longitudinal directions,
υ	is the poisson's ratio, and
$\sigma_\theta, \sigma_z, \sigma_r$	are the hoop, longitudinal & radial stresses.

References

[1] W. Flügge, Stresses in Shells, 2nd ed., Springer-Verlag, Berlin (1973).
[2] H. Kraus, Thin Elastic Shells, Wiley, New York (1972).
[3] S. Timoshenko and S. Woinowsky-Krieger, Theory of Plates and Shells, 2nd ed., McGraw-Hill, New York (1959).
[4] J.F. Harvey, Theory and Design of Pressure Vessels, Van Nostrand Reinhold N.Y (1991).
[5] E.L. Wilson and R.E. Nickell, "Application of the Finite Element Method to Heat Conduction Analysis", Nucl. Eng. Design, Vol. 4, pp. 276-286 (1966).
[6] R.H. Gallagher, "Problems and Progress in Thin Shell Finite Element Analysis", Applied Science Publisher LTD (1982).
[7] N.C. Knowles, A. Razzaque and J.B. Spooner, Experience of Finite Element Analysis of Shell Structure, Applied Science Publisher LTD (1982).
[8] S. Ahmed, B.M. Irons and O.C. Zienkiewicz, "Analysis of Thick and Thin

Shell Structures by Curved finite Element", International Journal of Numerical Methods in Engineering, Vol. 2, pp. 419-451 (1970).

[9] O.C. Zienkiewicz and R.L. Taylor, The Finite Element Method, McGraw-Hill (1989).

[10] O.C. Zienkiewicz, R.L. Taylor and J.M. Too, "Reduced Integration Technique in General Analysis of Plates and Shells", Journal of Numerical Methods in Engineering, Vol. 3, pp. 275-290 (1971).

[11] K.J. Han and P.L. Gould, "Quadrilateral Shell Element for Rotational Shells", Journal of Engineering Structure, Vol. 4, pp. 129-131 (1982).

[12] M.H. Fayed, "Stresses at the Intersection of Sphere and Cylinder by a Variant Finite Difference Method", Journal of Applied Mechanics (1974).

[13] L.A. Godoy and J.G. Croll, "Geometric Discontinuities in Thin Shell Finite Element Formulation", Journal of Computer and Structure, Vol. 14, pp. 37-41 (1981).

[14] O.C. Zienkiewicz and Y.K. Cheung, The Finite Element Method in Structural and Continuum Mechanics, McGraw-Hill, London and New York (1967).

[15] G. Warzee, "Finite Element Method and Laplace Transform- Comparative Solutions of Transient Heat Conduction Problems", Journal of Computer and Structure, Vol. 4, pp. 979-991 (1974).

[16] K.S. Surana and P. Kalim, "Isoparametric Axisymmetric Shell Elements with Temperature Gradients for Heat Conduction", Journal of Computer and Structure, Vol. 23, pp. 279-289 (1986).

[17] F. Cecari and L. Meneghini, "Transient Convective-Conductive Heat Transfer Problems in the PEC Fast Breeder Reactor Test Loop with Thermal Shocks on the Structure", Journal of Computer and Structure, Vol. 23, pp. 315-321 (1986).

[18] G. Duijvesign, J. Brichley and K. Reichlin, "Prediction of Thermoplastic Failure of a Reactor Pressure Vessel Under Postulated Core Melt Accident", Journal of Computer and Structure, Vol. 64, pp. 1239-1249 (1997).

[19] T. Vilhelmsen, "Reference Stress Solutions of Flat End to Cylinder Shell Connection and Comparison with Design Stresses Predicted y Codes", International Journal of Pressure Vessels and Piping, Vol. 77, pp. 35-39 (2000).

[20] M. Law, W. Payten and K. Snowden, "Modeling Creep of Pressure Vessels with Thermal Gradients Using Theta Projection Data", International Journal of Pressure Vessels and Piping, Vol. 79, pp. 847-851 (2002).

[21] M. Jabbaria, S. Sohrabpourb and M. R. Eslami, "Mechanical and Thermal Stresses in a Functionally Graded Hollow Cylinder Due to Radially Symmetric Loads", International Journal of Pressure Vessels and Piping, Vol. 79, pp. 493-497 (2002).

[22] K.D. Hagen, Heat Transfer With Applications, Prentice-Hall, Inc. (1999).

[23] H.H. Bendar, Pressure Vessel Design Handbook, VNR Company, New-York (1981).